THE JOURNAL OF PHYSICAL CHEMISTRY B

ARTICLE

pubs.acs.org/JPCB

Ab Initio Simulation of Changes in Geometry, Electronic Structure, and Gibbs Free Energy Caused by Dehydration of Hydrotalcites Containing Cl^- and CO_3^{2-} Counteranions

Deyse G. Costa,[†] Alexandre B. Rocha,[‡] Wladmir F. Souza,[§] Sandra Shirley X. Chiaro,[§] and Alexandre A. Leitão*[,†]

[†]Departamento de Qumica, Universidade Federal de Juiz de Fora, Juiz de Fora, MG, 36036-330, Brazil

[‡]Universidade Federal do Rio de Janeiro, Instituto de Qumica,Departamento de Fsico-Qumica, Av. Athos da Silveira Ramos, 149 Bloco A, Cidade Universitária, Rio de Janeiro, RJ, 21941-909, Brazil

[§]PETROBRAS-CENPES, Ilha do Fundão, Rio de Janeiro, RJ, 21941-915, Brazil

ABSTRACT: This ab initio study was performed to better understand the correlation between intercalated water molecules and layered double hydroxides (LDH), as well as the changes that occur by the dehydration process of Zn−Al hydrotalcite-like compounds containing Cl^- and CO_3^{2-} counterions. We have verified that the strong interaction among intercalated water molecules, cointercalated anions, and OH groups from hydroxyl layers is reflected in the thermal stability of these compounds. The $Zn_{2/3}Al_{1/3}(OH)_2Cl_{1/3}\cdot 2/3H_2O$ hydrotalcite loses all the intercalated water molecules around 125 °C, while the $Zn_{2/3}Al_{1/3}(OH)_2(CO_3)_{1/6}\cdot 4/6H_2O$ compound dehydrates at about 175 °C. These values are in good agreement with experimental data. The interlayer interactions were discussed on the basis of electron density difference analyses. Our calculation shows that the electron density in the interlayer region decreases during the dehydration process, inducing the migration of the Cl^- anion and the displacement of the hydroxyl layer from adjacent layers. Changes in these compound structures occur to recover part of the hydrogen bonds broken due to the removal of water molecules. It was observed that the chloride ion had initially a lower Löwdin charge ($Cl^{-0.43}$), which has increased its absolute value ($Cl^{-0.58}$) after the water molecules removal, while the charges on carbonate ions remain invariant, leading to the conclusion that the Cl^- anion can be more influenced by the amount of water molecules in the interlayer space than the CO_3^{2-} anion in hydrotalcite-like compounds.

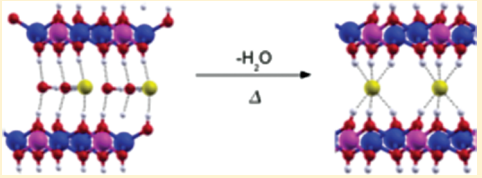

1. INTRODUCTION

Hydrotalcite-like compounds or layered double hydroxides (LDHs) have the general formula $[M_{1-x}Me_x(OH)_2]^{x+}(A^{n-})_{x/n}\cdot mH_2O$ and are formed by the stacking of positive hydroxide layers and hydrated A^{n-} interlayer counteranions. The interlayer anions and water molecules are usually labile. Therefore, these minerals exhibit anion exchange capacity, which allows them to be used in many applications.[1]

Although these minerals usually present water molecules in their crystalline structure, it is possible to obtain anhydrous LDH by heat treatment.[2] It is known that all the intercalated water molecules are removed at moderate temperature. However, due to their highly hygroscopic nature, the LDHs rehydrate at room temperature by adsorption of the water molecules from the atmosphere or solutions.[3] Water molecules contribute to stabilize the lamellar structure via a hydrogen bond involving anions and hydroxyl groups of the layers.[4−6]

Some properties of the hydrotalcite-like compounds, such as distances between layers, anion exchange power, and catalytic activity, can be influenced by the amount of water molecules present in their structures. The ^{35}Cl NMR experiments showed that the intercalated ClO_4^- and the Cl^- anions have significant differences in their vicinity depending on the degree of hydration.[7,8] The relative humidity also affects layer distances and interlayer dynamics of LDHs intercalated with Cl^-, Br^-, I^-, NO_3^-, ClO_4^-, SeO_4^{2-}, SO_4^{2-}, and MoO_4^{2-}. The same influence of water vapor pressure does not occur when the anions are F^-, OH^-, or CO_3^{2-}.[9]

As a consequence, hydrated forms of layered double hydroxides can be important in many processes and applications of these materials. Computer simulations can be used to understand the water−clay system at the microscopic level and to interpret experimental results. In spite of these facts, the number of ab initio calculations performed for hydrated[4,10,11] and for anhydrous[12−15] LDHs is still small. The correlation between the intercalated water molecules and the LDHs was investigated mainly by classical molecular dynamics,[5,6,16−21] in such a way that many aspects of the structure, energetics, and particularly reactions in the hydrated hydrotalcites are not understood.

Although the hydrotalcites form a class of hydrated minerals, the majority of DFT studies on these compounds was performed in their anhydrous forms. The main reason for that lies in the reduction of the computational cost, but this approach can

Received: November 8, 2010
Revised: February 17, 2011
Published: March 15, 2011

sometimes impair the resulting analyses, since the structure, the dynamics, and the stability of the intercalated species are influenced by their interactions with water molecules. In this work we investigated the geometrical and the electronic structure of $Zn_{2/3}Al_{1/3}(OH)_2Cl_{1/3}\cdot 2/3H_2O$ and $Zn_{2/3}Al_{1/3}(OH)_2(CO_3)_{1/6}\cdot 4/6H_2O$ and their dehydrated forms $Zn_{2/3}Al_{1/3}(OH)_2Cl_{1/3}$ and $Zn_{2/3}Al_{1/3}(OH)_2(CO_3)_{1/6}$. All of them are in $3R_1$ polytype and are named Zn−Al−Cl, Zn−Al−CO_3, D-Zn−Al−Cl, and D-Zn−Al−CO_3, respectively. The dehydration Gibbs free energies were calculated as well as the dehydration temperature of Zn−Al−Cl and Zn−Al−CO_3.

2. THEORETICAL METHODOLOGY

On the basis of experimental investigations,[22,23] we have assumed the validity of the total Zn−Al ordering. This allows us to use supercells represented by $(\sqrt{3} \times \sqrt{3})R30°$ and $(2\sqrt{3} \times \sqrt{3})R30°$ reconstructions of brucite-like layers as shown in our previous paper.[4] The interlayer structure was built with anions and water molecules at specific prismatic sites between hydroxyl sheets.

All calculations were performed using PWscf, a DFT code based on plane waves.[24] The energy cutoff for the plane-wave basis employed was 40 Ry (240 Ry for the density), and we adopted the PBE exchange correlation functional in the generalized gradient approximation.[25] Ultrasoft potentials were used to describe the nuclear core and inner electrons.[26] Monkhorst−Pack[27] meshes of 3 × 3 × 2 and 2 × 3 × 2 k-point sampling in the first Brillouin Zone were used for $(\sqrt{3} \times \sqrt{3})R30°$ and $(2\sqrt{3} \times \sqrt{3})R30°$ supercells, respectively. These choices were found to be suitable to have total energies and stress tensors well converged.

Each supercell had two water molecules per Al, to obtain equivalent hydration for Zn−Al−Cl and Zn−Al−CO_3 compounds. Our model was built from a single layer to reduce the number of atoms. The stacking sequence is recovered by a sloped c vector.[4] Although these supercells are very simple, their construction allows us to recover the $3R_1$ polytype by using the periodic boundary conditions. The guest species were located at the middle point between consecutive layers. The O atoms of the water molecules and the Cl^- ions were located near the H atoms of the OH groups since they were expected to interact by hydrogen bonds. The CO_3^{2-} anion was set parallel to the hydroxide layers at the trigonal prismatic site being coordinated to 6OH by hydrogen bonds, three from either side of the interlayer (see Figure 2). These settings reproduce the $R\bar{3}m$ space group, which is the one reported for these LDHs.[19,28]

All cell parameters, a, b, c, α, β, and γ, and nuclei positions were optimized. The dehydrated compounds D-Zn−Al−Cl and D-Zn−Al−CO_3 were built by removing water molecules of the optimized Zn−Al−Cl and Zn−Al−CO_3 and by proceeding with new full geometric optimization. Equilibrium lattice parameters and ion positions for all the structures were relaxed until all force components were smaller than 0.001 Ry/Bohr. Full vibrational calculations were performed, and their analyses were used to validate the optimized geometries as real minima. The vibrational data were also used to calculate both the contribution of lattice thermal vibration to total energy and the zero point energy (ZPE). In the vibrational calculations, only the γ-point was used.

The chemical equation used to calculate the energy associated with dehydration is shown below

$$Zn_{2/3}Al_{1/3}(OH)_2(A^{n-})_{x/n}\cdot mH_2O(s) \rightarrow Zn_{2/3}Al_{1/3}(OH)_2(A^{n-})_{x/n}(s) + mH_2O(g)$$

where A^{n-} is either Cl^- or CO_3^{2-} anions.

The enthalpy, entropy, and Gibbs free energy of the reactions were calculated using the following equations

$$\Delta H(T) = ((H_{dehyd} + mH_W) - H_{hyd})/N_{Al+Mg} \quad (1)$$

$$\Delta S(T) = ((S_{dehyd} + mS_W) - S_{hyd})/N_{Al+Zn} \quad (2)$$

$$\Delta G = ((G_{dehyd} + mG_W) - G_{hyd})/N_{Al+Zn} \quad (3)$$

where H_{dehyd}, S_{dehyd}, G_{dehyd}, H_{hyd}, S_{hyd}, and G_{hyd} are the enthalpy, entropy, and Gibbs free energy calculated for anhydrous and hydrated LDHs, respectively. H_W, S_W, and G_W are the enthalpy, entropy, and Gibbs free energy calculated for gaseous water molecules. N_{Al+Zn} is the number of cations in the supercell.

To study the reaction at increasing temperatures, we have calculated the difference in thermodynamic properties such as enthalpy (ΔH), entropy (ΔS), and Gibbs free energy (ΔG) of the reaction from 25 to 275 °C at 1 atm. Thermal correction to enthalpy and entropy includes effects of vibration at each temperature. Zero-point vibrational energy was considered for the crystals, as shown in eqs 4 and 5, respectively.

$$H(T) = E^{elec} + E^{ZPE} + E^{vib}(T) \quad (4)$$

where E^{elec} is the total electronic energy at 0 K; E^{ZPE} is the zero-point vibrational energy which is a linear sum of the fundamental harmonic frequencies; and $E^{vib}(T)$ is the vibrational contribution.

$$S(T) = S^{conf} + S^{vib}(T) \quad (5)$$

where S^{conf} and $S^{vib}(T)$ are the configurational and vibrational entropy, respectively.

The vibrational energy, within harmonic approximation, is given by

$$E^{vib}(T) = \sum_{i=1}^{3N-3} \left[\frac{\hbar\omega_i}{\exp\left(\frac{\hbar\omega_i}{k_B T}\right) - 1} \right] \quad (6)$$

where N is the number of atoms in the unit cell; i is the index of vibrational mode; $\hbar\omega_i$ is the vibrational energy of mode i; and k_B is the Boltzmann constant.

The configurational entropy, for conformations of water molecules, guest anions, and vacancies in the interlayer, and the vibrational entropy, within harmonic approximation, are given by eqs 7 and 8, respectively

$$S^{conf} = -RN_T[X_A \ln X_A + X_W \ln X_W + X_V \ln X_V] \quad (7)$$

where N_T is the total moles of mixing species; and X_A, X_W, and X_V are the mole fraction of anion, water molecule, and vacancy, respectively. This equation was proposed by Allada.[29]

$$S^{vib}(T) = k_B \sum_{i=1}^{3N-3} \left[\frac{\hbar\omega_i}{k_B T}\left(\exp\left(\frac{\hbar\omega_i}{k_B T}\right) - 1 \right)^{-1} - \ln\left(1 - \exp\left(\frac{-\hbar\omega_i}{k_B T}\right)\right) \right] \quad (8)$$

For thermodynamic properties of the gaseous water molecules, the translational and rotation contributions must also be

dx.doi.org/10.1021/jp110668s |J. Phys. Chem. B 2011, 115, 3531–3537

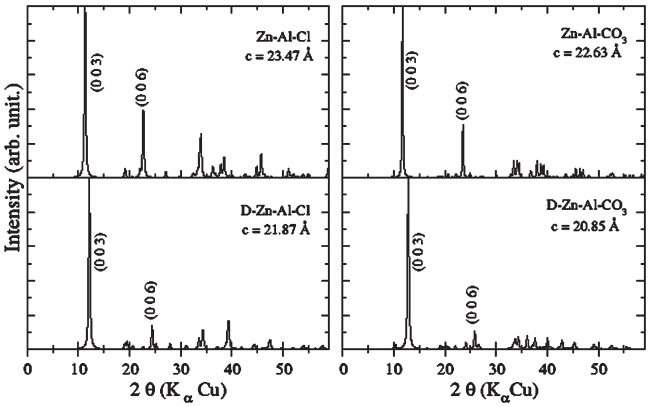

Figure 1. Simulated XRD data for hydrated and dehydrated Zn−Al−Cl and Zn−Al−CO_3.

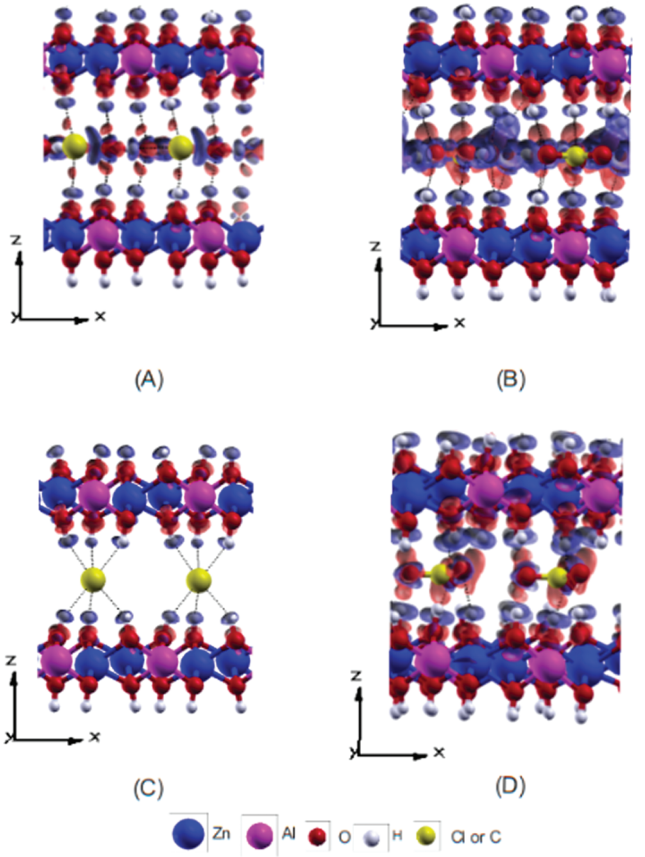

Figure 2. Charge density difference of (A) Zn−Al−Cl, (B) Zn−Al−CO_3, (C) D-Zn−Al−Cl, and (D) D-Zn−Al−CO_3. The blue region presents the depletion of charge density, and the red region indicates the increase of charge density. The contour spacing is 0.003 electrons/Bohr^3.

considered. Thus, we can rewrite the expressions 4 and 5 as

$$H(T) = E^{elec} + E^{ZPE} + E^{vib}(T) + E^{rot}(T) + E^{trans}(T) + RT \quad (9)$$

where $E^{trans}(T)$ and $E^{rot}(T)$ are the translational and rotational contributions to the enthalpy, respectively. They are equivalent to 3/2RT, and R is the gas constant. RT is equivalent to the PV term, that is necessary to obtain the enthalpy of a gas.

$$S(p,T) = S^{vib}(T) + S^{rot}(T) + S^{trans}(p,T) \quad (10)$$

The rotational and the translational entropy, within the ideal-gas approximation, are given by

$$S^{rot}(T) = k_B\left\{\ln\left[\frac{\sqrt{\pi I_A I_B I_C}}{\sigma}\left(\frac{8\pi^2 k_B T}{h^2}\right)^{3/2}\right] + 3/2\right\} \quad (11)$$

where I_A, I_B, and I_C are the moments of inertia of the molecule. σ is the symmetry number of the molecule, and T is the absolute temperature. k_B and h are the Boltzmann and Plank constant, respectively.

$$S^{trans}(p,T) = k_B\left\{\ln\left[\left(\frac{2\pi M k_B T}{h^2}\right)^{3/2}\frac{k_B T}{p}\right] + 5/2\right\} \quad (12)$$

where p is the pressure and M is the molecular mass.

Thus, we can calculate the Gibbs free energy by

$$\Delta G = \Delta H - T\Delta S \quad (13)$$

All the molecular graphics have been generated by the XCRYSDEN graphical package,[30,31] and the X-ray powder diffractograms have been obtained by using Mercury software.[32]

3. RESULTS AND DISCUSSION

We have obtained good agreement between the simulated and the experimental lattice parameters for both Zn−Al−Cl and Zn−Al−CO_3 LDHs, as can be seen in Table 1. The simulated XRD patterns (Figure 1) of these materials exhibit the typical layered features. The c parameter is 23.474 Å for Zn−Al−Cl and 22.631 Å for Zn−Al−CO_3 LDHs, quite similar to those reported in experimental works.[19,28,33,34] GGA functionals tend to overestimate the unit cell parameters because the van der Waals interactions are not properly described. Thus, our calculated cell parameters are larger than the experimental data (Table 1). Nevertheless, our error is very small because the LDHs consist of positively charged hydroxyl layers that are charge balanced by hydrated anions in the interlayer regions, and the interactions responsible for the lamellar packing are mainly Coulombian and hydrogen bond.[4] The discrepancy between the theoretical calculation and the experimental measure was approximately 2% for the a parameter and 0.5% for the c parameter.

When the water molecules are removed, the layered structure of LDH is not destroyed, and their hexagonal lattice structure is kept almost unaltered, as can be seen in Table 1. The optimized angles α, β, and γ were 89°, 90°, and 120° and 84°, 89°, and 120° to dehydrated minerals, D-Zn−Al−Cl and D-Zn−Al−CO_3, respectively. The absence of water molecules has little effect on the a unit cell parameter, but a contraction of the c-axis about 3.6% and 5.0% was observed for D-Zn−Al−Cl and D-Zn−Al−CO_3, respectively (Table 1).

The simulated XRD patterns (Figure 1) corroborate these results through prominent (00l) reflections seen below $2\theta = 30°$, which are indicators of layered solids. It was observed, after the water molecule removal, that the (003) and the (006) peaks have been shifted toward high angles, relative to Zn−Al−Cl and Zn−Al−CO_3, indicating a reduction of the interlayer spacing of materials. The (00l) peak shift was the most significant change

Table 1. Main Geometrical Parameters for Zn−Al−Cl, Zn−Al−CO_3, D-Zn−Al−Cl, and D-−Zn−Al−CO_3 LDHs

	Zn−Al−Cl		D−Zn−Al-Cl	Zn−Al−CO_3		D−Zn−Al-CO_3
	exp.[a]	theo.	theo.	exp.[a]	theo.	theo.
a/Å	3.0813(3)	3.1300	3.1069	3.0737(1)	3.0040	3.0992
c/Å	23.351(5)	23.474	21.867	22.743(2)	22.631	20.852
α/°	90.0	88.6	89.7	90.0	90.1	84.3
β/°	90.0	90.7	90.3	90.0	91.0	89.3
γ/°	120.0	120.0	120.2	120.0	119.4	121.3
M−OH /Å	2.054	2.070	2.665	2.034	2.003	2.049
$(OH-OH)_{sharededges}$/Å	2.715	2.743	-	2.665	2.715	2.665
$(H_2O,A^-)-(H_2O,A^-)$/Å	-	2.924	-	2.861	2.805	-
∠(OH)−(M)−(OH)/°	82.78	82.0	96.34	81.86	82.50	99.57
∠O−C−O/°	-	-	-	120.01	120.01	120.00
C−O/Å	-	-	-	1.170	1.300	1.306

[a] Ref 28. We reported mean theoretical values for (OH−OH) and $(H_2O,A^-)-(H_2O,A^-)$.

observed in the diffractogram of the anhydrous compounds in relation to the original hydrated LDH.

In a typical hydrated LDH, it was reported that the interaction of water molecules with the rest of the structure makes the interlayer a well-structured region.[35−39] The species confined in this region have their mobility restricted. In these compounds, the interactions among water molecules are intermediate between that in ice Ih and that found in liquid water.[4,7,8,20,35] This characteristic is consistent with the occurrence of high charge transfer in both hydrated LDHs, as shown in Figures 2A and 2B, in which the isosurfaces in 3D space are red or blue when $\Delta\rho(\vec{r})$ assumes values of −0.003 and 0.003 electron/Bohr^3, respectively. In both cases, the anions form a H bond with the OH-layer and H_2O. Of course, water molecules interact strongly with one another. Thus, hydrogen bonds do not occur as isolated entities, but they appear as extended hydrogen bond networks. On the other hand, when water molecules are removed, a decrease of charge transfer is observed (Figures 2C and 2D). This indicates that the structure of this hydrogen bond network varies greatly with the anion composition and the amount of water molecules present, and they can play an important role in controlling both the lattice expansion and the interlayer dynamics.

When water molecules are removed, vacant positions are generated close to the anions, allowing their migration. By comparing Figures 3A and 3B, it can be seen that the Cl^- was moved from the corner to the center of the prismatic site in D-Zn−Al−Cl. In the case of LDH with CO_3^{2-}, Figures 3C and 3D show that this anion was kept at the same site after the dehydration process. These results indicate that after the breaking of hydrogen bonds, due to water molecule removal, the system reacts to reestablish completely or partially the hydrogen bonds. As a result, it is possible to observe an anion migration or a layer distortion and, also, a contraction of basal spacing.

The material D-Zn−Al−CO_3 exhibits higher charge transfer in comparison to D-Zn−Al−Cl. This result is related to the trigonal planar geometry of the carbonate anions, which favors the formation of strong hydrogen bonds both with hydroxyl groups of hydroxide layers and with the cointercalated water molecules. If a certain number of hydrogen bonds are broken due to removal of water molecules, there still rests a strong interaction between the anion and the layer. Moreover, a fraction of broken hydrogen bonds due to the removal of water molecules

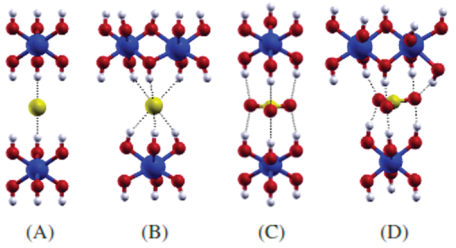

Figure 3. (A) Cl^- at the corner of the prismatic site in Zn−Al−Cl, (B) Cl^- at the center of the prismatic site in D-Zn−Al−Cl, (C) CO_3^{2-} occupying the prismatic site in Zn−Al−CO_3, and (D) CO_3^{2-} occupying the prismatic site in D-Zn−Al−CO_3.

can be recovered with a small layer dislocation (Figure 3D), which provides a degree of stacking disorder but does not substantially alter its structure.

For the D-Zn−Al−Cl LDH, the anion was moved to the hydroxyl prismatic center (the same site occupied by the C atom from CO_3^{2-}), which is a symmetric site, resulting in a significant structural reorganization of the interlayer. Thus, the intercalated water molecules not only are associated with basal spacing but also are the responsible species for the interaction between hydroxide layers. Their removal can favor the slipping of layers leading to the appearance of stacking faults and polytype change.

The migration of Cl^- can give us insight into the mechanism of anion removal from the interlayer region. This migration takes place close to the hydrogen atom of hydroxide layers, which could make the release of HCl easier upon thermal decomposition of the Zn−Al−Cl, as reported by Velu et al.[34] Moreover, the halide migration and the reordering of the interlayer region, as a function of dehydration progress, were observed in some experimental studies.[40,41] Similarly, NMR experiments have shown that the Cl^- anion, in different hydration states, changes its feature. The same is not true for the CO_3^{2-} anion.[8,9]

These results show that the interactions in the interlayer region change significantly when the LDH is dehydrated. The hydroxide layers displace to allow the formation of interactions by which anions are stabilized, as in the case of CO_3^{2-}, or the guest can move toward a different position, in which it can obtain a higher coordination number, as in the case of the Cl^- anion. In both

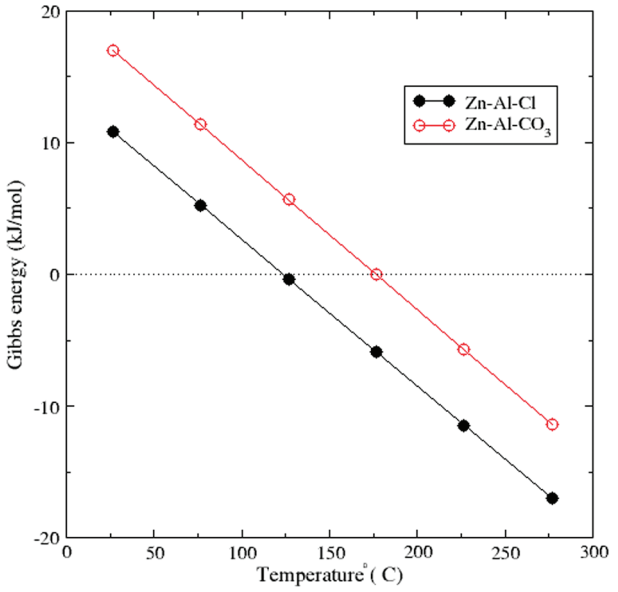

Figure 4. Dependence between the Gibbs energy and temperature to complete dehydration of Zn−Al−Cl and Zn−Al−CO_3.

cases, changes occur to maximize the hydrogen bonds in the interlayer region as well as to stabilize the layered structure in the absence of intercalated water molecules. In this work, the hydrated and dried LDHs were analyzed. There may be intermediate structures of partially hydrated mineral, but these were not studied here.

The total amount of water molecules in the LDHs varies depending on the environmental conditions such as temperature and external pressure or on the synthetic route used for their preparation. The variation of the Gibbs free energies (Figure 4), associated with the reaction shown in Section 2, is positive for both hydrotalcite-like compounds at low temperatures. This shows that this reaction is not expected to be spontaneous at these conditions. It is coherent with the fact that, at room temperature, these LDHs are found in their hydrated form. We have found a linear correlation between Gibbs free energies and temperature, and as expected, when the temperature increases the dehydrated forms become the stable forms of these minerals.

ZPE gives an important contribution to the energy of all the systems. The ZPE variation, ΔZPE, is around −7.81 and −8.68 kJ/mol for the dehydration reaction of Zn−Al−Cl and Zn−Al−CO_3, respectively. For Zn−Al−Cl, the ΔH varies from 44.37 to 43.58 kJ/mol for 25 °C and 275 °C, respectively, the reaction being considered endothermic. For the same temperature range, the corresponding ΔH for Zn−Al−CO_3 is 51.09 and 50.64 kJ/mol. This indicates that the spontaneity of the dehydration reaction is controlled by the entropy term, $T\Delta S$. The entropy increases drastically due to the evolution of the gas molecules (with translational and rotational degrees of freedom); consequently, the high temperature will increase the entropy factor $T\Delta S$ to a large extent, and $\Delta G = \Delta H - T\Delta S$ may become negative. For 25 °C and 275 °C, the calculated $T\Delta S$ was 33.63 and 63.42 kJ/mol for Zn−Al−Cl and 34.04 and 61.83 kJ/mol for Zn−Al−CO_3 LDH. These $T\Delta S$ values suggest a large contribution of rotational and translational entropy of water molecules. To the range of 25−275 °C, the TS term, considering only the rotational entropy, varies from 11.45 to 23.82 kJ/mol, while using only the translational entropy the values are 28.77−7.53 kJ/mol, respectively. The vibrational entropy contribution of the TS term of water molecules is less than 0.4 kJ/mol, and it does not contribute significantly to the energy calculation. On the other hand, the water molecules leave the LDH structure during the reaction, and the effect in the $T\Delta S$ term, considering only the vibration, is 6.59−17.93 kJ/mol for Zn−Al−Cl and 6.18−19.52 kJ/mol for Zn−Al−CO_3.

The minimum temperature to have fully dehydrated Zn−Al−Cl was evaluated at 125 °C, while for Zn−Al−CO_3 that was 175 °C. These values are in good agreement with experimental data, which have reported that Zn−Al−Cl dehydrates between 127 and 130 °C and Zn−Al−CO_3 at 166 °C,[33,34] confirming the consistency of our model. The high heat of vaporization of water molecules in the LDH, compared to liquid water, can be attributed to the presence of strong intermolecular hydrogen bonding, which provides additional attractive forces between the molecules and affects the properties that depend on intramolecular forces. The energy required to break multiple hydrogen bonds explains this high heat of vaporization. The dehydration energy calculated in this way is a useful parameter for predicting relative thermodynamic stability of hydrated layered materials, confirming the experimental observation that dried LDHs are very hygroscopic materials.

To understand the redistribution of the electron density at the interlayer region, we have calculated the total and projected density of states, DOS and pDOS (Figure 5). The Fermi energy level was set at 0 eV. The total DOS have distinct energy gaps between the top of the valence band and the bottom of the conduction band for Zn−Al−CO_3 and D-Zn−Al−CO_3 LDHs, which are 3.4 and 2.1 eV, respectively, while for Zn−Al−Cl and D-Zn−Al−Cl a gap value of 3.8 eV was found. For D-Zn−Al−CO_3 LDH, the bottom of the conduction band is closer to the Fermi level than the bottom of the conduction band of Zn−Al−CO_3 LDH. This is an indication of the increase of the acidity of the former compound, so their conduction bands are available to interact with Lewis bases such as H_2O molecules. The calculated results of the band gap are probably smaller than the experimental value, due to the typical underestimation of the band gap for DFT, but they are at least qualitatively correct.

As can be seen in Figure 5 (black line), the dehydration of LDHs was accompanied by a reduction in the number of valence electrons, but the basic features of DOS are shared by all phases. This indicates that the orbital contributions from hydroxyl layers dominate the overall shape of the total DOS. To investigate the chemical bonding of intercalated species and verify how the absence of water molecules affects the electron density of the interlayer region, we calculated the partial density of states (pDOS) of anions inserted into LDHs. This result was presented in Figure 5 (red line). The pDOS for the CO_3^{2-} anion in D-Zn−Al−CO_3 LDH does not change compared with that of Zn−Al−CO_3 LDH. On the other hand, a comparison of the Cl^- anion pDOS of D-Zn−Al−Cl and of Zn−Al−Cl LDH showed that the former was shifted by about 1.2 eV toward the Fermi energy. These results are consistent with the ^{35}Cl NMR experiments[8,9] and our observation for the calculated geometry and the density charge difference analyses, in which the intercalated Cl^- anion changes its feature in different hydration states, in contrast with the intercalated CO_3^{2-} anion.

The Löwdin charges, shown in Table 2, confirm this observation. From population analysis, it was observed that the chloride ion was less ionic ($Cl^{-0.43}$) and became more ionic ($Cl^{-0.58}$) after water molecule removal. In typical LDHs, the electron transfer

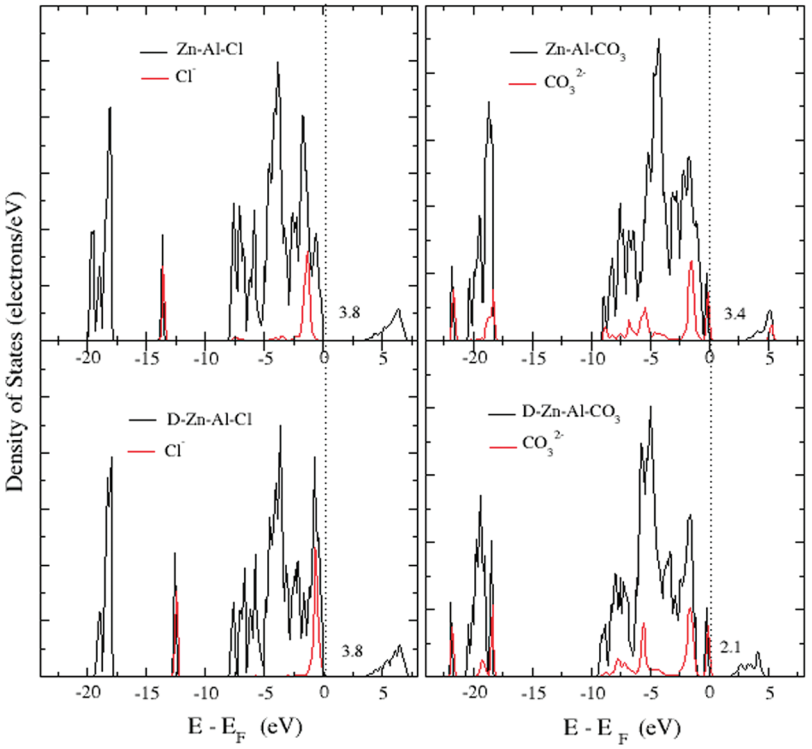

Figure 5. Density of states (DOS) of hydrated and dehydrated Zn−Al−Cl and Zn−Al−CO_3. The red line indicates the projected density of states (PDOS) of intercalated anions. The Fermi level is chosen as zero energy level for these plots, and it is indicated by vertical dashed lines.

Table 2. Löwdin Charges ($|e^-|$) of LDHs

	Zn−Al−Cl	D-Zn−Al−Cl	Zn−Al−CO_3	D-Zn−Al−CO_3
Al	1.14	1.14	1.14	1.14
Zn	1.48	1.48	1.48	1.48
O	−0.86	−0.86	−0.86	−0.86
H	0.35	0.38	0.38	0.38
Cl	−0.43	−0.58	-	-
O_{water}	−0.67	-	−0.67	-
H_{water}	0.36	-	0.38	-
C	-	-	0.67	0.67
O_{anion}	-	-	−0.54	−0.54

direction is from anion toward hydroxyl layers and toward water molecules (Figure 2). Thus, the increase of Cl charge indicates that the electrons transfer was less pronounced in the dehydration, while the charges of carbonate ions remain invariant in consequence of the enhancement of Coulombic interactions between the intercalated anion and the hydroxide layer.

We have found that the electronic structure change in Zn−Al−Cl occurs near the top of the valence band of the material (Figure 5). Then, this can also be confirmed by the calculated square modulus of the valence band in Figure 6. For hydrated materials, the square modulus of the valence band is dominated by the contribution of molecular orbitals of hydroxyl groups (Figure 6A). For the dehydrated compound, an additional contribution of chloride orbitals was observed (Figure 6B). This last result has already been found by other ab initio calculations performed without water molecules.[13,15] This means that D-Zn−Al−Cl reacting with acid species (proton donors) will interact with both hydroxyl groups and chloride anions because the basicity is

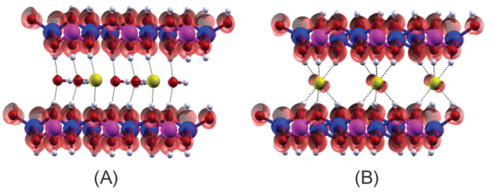

Figure 6. Plots of calculated square modulus of valence of (A) hydrated and (B) anhydrous Zn−Al−Cl. Isodensity surface is 0.001 electrons/$Bohr^3$ in both cases.

proportional to the charge density and the charge transfer processes are accomplished via the frontier states. The presence of different active sites for these solid bases can affect the selectivity in catalysis and their adsorption properties, favoring or hindering certain reactions. In this case, many investigations can be affected when the model used is not able to account for the detailed electronic structure of LDH and their chemical interactions.

4. CONCLUSIONS

In this work, we have investigated the changes in geometrical and electronic structure of Zn−Al−Cl and Zn−Al−CO_3 hydrotalcites and their dehydrated forms D-Zn−Al−Cl and D-Zn−Al−CO_3. Thermodynamics of the dehydration reaction was also calculated. The dehydration process is accompanied by a decrease in basal spacing. The contraction of the *c*-axis was at about 3.6% and 5.0% for D-Zn−Al−Cl and D-Zn−Al−CO_3 LDHs, respectively, whereas the *a* unit cell parameters are almost not affected. The ab initio calculations have shown that the water molecules in the interlayer play an important role in the stability of the layered structure since it acts cooperatively to maximize

dx.doi.org/10.1021/jp110668s |*J. Phys. Chem. B* 2011, 115, 3531–3537

the hydrogen bonding between the layers and the intercalated species, as was observed in the electron density difference analyses. The strong interactions are reflected in the high temperature of dehydration. Zn−Al−Cl loses its water molecules at about 125 °C, and for Zn−Al−CO_3 LDH the same process was calculated to occur at 175 °C. These temperatures mark the complete removal of the water molecules of these minerals, but the layered brucite-like structure is retained.

The H_2O removal leads to a decrease of interaction between the layers and the intercalated species, favoring the dynamics of the guest and the slipping features of the layers. The most significant changes were observed for the Cl^- anion. It migrates from the corner to the center of the prismatic site in D-Zn−Al−Cl. This shift is also associated with the change of their chemical environment since it was observed that the chloride ion was less ionic ($Cl^{-0.43}$) and became more ionic ($Cl^{-0.58}$) after water molecule removal. The same analysis done to carbonate ions showed that it remains invariant. We can conclude that the dehydrated model is appropriate to investigate LDH intercalated with some anions, but it fails in other cases. In addition, our calculations have indicated that the influence of water molecules is more pronounced in hydrotalcite-like compounds in which the electron transfer is relatively low.

AUTHOR INFORMATION

Corresponding Author
*E-mail: alexandre.leitao@ufjf.edu.br.

ACKNOWLEDGMENT

We thank CNPq (Conselho Nacional de Desenvolvimento Cientfico e Tecnológico), FAPEMIG (Fundação de Amparo à Pesquisa do Estado de Minas Gerais), FAPERJ, and Petrobras SA for financial support during this work.

REFERENCES

(1) Crepaldi, E. L.; Valim, J. B. *Quim. Nova* **1998**, *21* (3), 300.
(2) Besserguenev, A. V.; Fogg, A. M.; Francis, R. J.; Price, S. J.; O'Hare, D. *Chem. Mater.* **1997**, *9*, 241.
(3) Petrova, N.; Mizota, T.; Stanimirova, Ts.; Kirov, G. *Microporous Mesoporous Mater.* **2003**, *63*, 139.
(4) Costa, D. G.; Rocha, A. B.; Souza, W. F.; Chiaro, S. S. X.; Leitão, A. A. *J. Phys. Chem. C* **2010**, *114*, 14133.
(5) Kim, N.; Harale; Tsotsis, T. T.; Sahimi, M. *J. Chem. Phys.* **2007**, *127*, 224701.
(6) Wang, J.; Kalinichev, G.; Kirkpatrick, R. J.; Hou, X. *Chem. Mater.* **2001**, *13*, 145.
(7) Hou, X.; Kirkpatrick, R. J. *Chem. Mater.* **2002**, *14*, 1195.
(8) Hou, X.; Kalinichev, A. G.; Kirkpatrick, R. J. *Chem. Mater.* **2002**, *14*, 2078.
(9) Hou, X.; Bish, D. L.; Wang, S. L.; Johnston, C. T.; Kirkpatrick, R. J. *Am. Mineral.* **2003**, *88*, 167.
(10) Qian, X.; Zhe-Ming, N.; Guo-Xiang, P.; Li-Tao, C.; Ting, L. *Acta Phys. -Chim. Sin.* **2008**, *24* (4), 601–606.
(11) Zhen-Ming, N.; Qian, X.; Ping, Y.; Jiang-Hong, M.; Xian-Ming, L. *Acta Phys. -Chim. Sin.* **2009**, *25* (11), 2325–2328.
(12) Costa, D. G.; Rocha, A. B.; Souza, W. F.; Chiaro, S. S. X.; Leitao, A. A. *J. Phys. Chem. C* **2008**, *112*, 10681.
(13) Trave, A.; Selloni, A.; Gourst, A.; Tichit, D.; Weber, J. *J. Phys. Chem. B* **2002**, *106*, 12291.
(14) Greenwell, H. C.; Stackhouse, S.; Coveney, P. V.; Jones, W. *J. Phys. Chem. B* **2003**, *107*, 3476.
(15) Xu, Q.; Ni, Z-m; Mao, J-h. *J. Mol. Struct.: Theochem.* **2009**, *762*, 1.
(16) Tran, P.; Smith, S.; Zhang, H.; Xu, Z. P.; Wong, Y.; Lu, G. Q. *J. Phys. Chem. Solids* **2008**, *69*, 1044.
(17) Li, H.; Ma, J.; Evans, D. G.; Zhou, T.; Li, F.; Duan, X. *Chem. Mater.* **2006**, *18*, 4405.
(18) Kim, N.; Kim, N.; Tsotsis, T. T.; Sahimi, M. *J. Chem. Phys.* **2005**, *122*, 214713.
(19) Lombardo, G. M.; Papalardo, G. C.; Punzo, F.; Constantino, F.; Constantino, U.; Sisani, M. *Eur. J. Inorg. Chem.* **2005**, 5026.
(20) Kirkpatrick, R. J.; Kalinichev, A. G.; Wang, J. *Mineral. Mag.* **2005**, *69* (3), 289.
(21) Lombardo, G. M.; Papalardo, G. C.; Punzo, F.; Constantino, F.; Constantino, U.; Sisani, M. *Chem. Mater.* **2008**, *20*, 5585.
(22) Sideris, P. J.; Nielsen, U. G.; Gan, Z.; Grey, C. P. *Science* **2008**, *321*, 113.
(23) Hines, D. R.; Solin, S. A. *Phys. Rev. B* **2000**, *61* (17), 11348.
(24) Baroni, S.; Dal Corso, A.; Gironcoli, de S.; Giannozzi, P. 2001. Available from: http://www.pwscf.org/.
(25) Perdew, J. P.; Burke, K.; Ernzerhof, M. *Phys. Rev. Lett.* **1996**, *77*, 3865.
(26) Vanderbilt, D. *Phys. Rev. B* **1990**, *41*, 7892.
(27) Monkhorst, H. J.; Pack, J. D. *Phys. Rev. B* **1976**, *13*, 5188.
(28) Radha, A. V.; Kamath, P. V.; Shivakumara, C. *J. Phys. Chem. B* **2007**, *111*, 3411.
(29) Allada, R. K.; Navrotsky, A.; Boerio-Goates, J. *Am. Mineral.* **2005**, *90*, 329.
(30) Kokalj, A. *J. Mol. Graphics Modell.* **1999**, *17*, 176.
(31) Kokalj, A.; Causà, M. *XCrySDen: (X-window) CRYstaline Strutures and DENsities*, 2003. Available from http://www.xcrysden.org.
(32) http://www.ccdc.cam.ac.uk.
(33) Vieira, A. C.; Moreira, R. L.; Dias, A. *J. Phys. Chem. C* **2009**, *113*, 13358.
(34) Velu, S.; Ramkumar, V.; Narayanan, A.; Swamy, C. S. *J. Mater. Sci.* **1997**, *32*, 957.
(35) Frost, R. L.; Weier, M. L.; Kloprogge, J. T. *J. Raman Spectrosc.* **2003**, *34*, 760.
(36) Frost, R. L.; Martens, W.; Ding, Z.; Kloprogge, J. T.; Therese, E. J. *Spectrochim. Acta* **2003**, *59*, 291.
(37) Frost, R. L.; Weier, M. L.; Clissold, M. E.; Williams, P. A. *Spectrochim. Acta A: Mol. Biomol. Spectrosc.* **2003**, *59*, 3313.
(38) Frost, R. L.; Weier, M. L.; Clissold, M. E.; Williams, P. A.; Kloprogge, J. T. *Thermochim. Acta* **2003**, *407*, 1.
(39) Frost, R. L.; Martens, W. N.; Duong, L.; Kloprogge, j. T. *J. Mater. Sci. Lett.* **2002**, *21*, 1237.
(40) Thomas, G. S.; Kamath, P. K.; Kannan, S. *J. Phys. Chem. C* **2007**, *111*, 18980.
(41) Prasanna, S. V.; Radha, A. V.; Kamath, P. V.; Kannan, S. *Clays Clay Miner.* **2009**, *57* (1), 82.